Effect of tin on poly(L-lactic acid) pyrolysis

Effect of Sn Atom on Poly(L-lactic acid) Pyrolysis

Haruo Nishida[a,*], Tomokazu Mori[a,b], Shinya Hoshihara[a], Yujiang Fan[a,c], Yoshihito Shirai[c], and Takeshi Endo[a,d]

[a] Molecular Engineering Institute, Kinki University, Fukuoka 820-8555, Japan

[b] Faculty of Computer Science and Systems Engineering, Kyushu Institute of Technology, Fukuoka, 820-8502, Japan

[c] Graduate School of Life Science and Systems Engineering, Kyushu Institute of Technology, Fukuoka 808-0196, Japan

[d] Faculty of Engineering, Yamagata University, Yamagata 992-8510, Japan

*Corresponding author

Haruo Nishida

Molecular Engineering Institute, Kinki University, Fukuoka 820-8555, Japan

Tel / Fax: +81-948-22-5706.

E-mail address: hnishida@mol-eng.fuk.kindai.ac.jp (H. Nishida)

Abstract

Sn 2-ethylhexanoate is an indispensable component of commercially available poly(L-lactic acid) (PLLA). However, the thermal degradation kinetics of PLLA containing the Sn atom has not yet clearly been established, in particular, whether the degradation mechanism is a 1st-order reaction or a random reaction. To clarify the effects of residual Sn atoms on the PLLA pyrolysis, PLLA samples with different Sn contents from 20-607 ppm were prepared and subjected to the pyrolysis with pyrolysis-gas chromatography/mass spectroscopy (Py-GC/MS) and thermobalance (TG). The pyrolysis of PLLA Sn-607 (Sn content: 607 ppm) with Py-GC/MS in the temperature range of 40-400°C produced lactides selectively. In contrast, the pyrolysis of PLLA Sn-20 (Sn content: 20 ppm) was accompanied by the production of cyclic oligomers. The dynamic pyrolysis of PLLA-Sn samples with TG clearly indicated that with an increase in Sn content there was a shift to a lower degradation temperature range and a decrease in activation energy *Ea*. The kinetic analysis of the dynamic pyrolysis data indicates that the Sn-catalyzed pyrolysis starts through a random degradation behavior and then shifts to a zero-order weight loss process as the main process. Three reactions were put forward as being possible mechanisms of the zero-order weight loss process; one being an unzipping reaction accompanying a random transesterification, the other two being the Sn-catalyzed pseudo-selective and selective lactide elimination reactions from a random position on a polymer chain. The obtained kinetic parameter values could be adequately explained for each degradation process.

Keywords:

poly(L-lactic acid), poly(L-lactide), PLLA, pyrolysis, thermal decomposition, kinetics, simulation, thermogravimetric analysis, random degradation, zero-order reaction

1. Introduction

Poly(L-lactic acid) [poly(L-lactide), PLLA] is a well-known biodegradable polymer. It has received much interest for its medical, pharmaceutical, and environmental applications [1-3]. Nowadays, because of its many useful properties, such as mechanical strength, transparency, and compostability [4-6], PLLA and its related copolymers are attracting much attention as promising alternatives to the commodity resins [7]. PLLA is generally prepared by the ring-opening polymerization of L,L-lactide [8,9], and the thermal degradation of PLLA results in the recovery of L,L-lactide [10,11]. Thus, this chemical property makes PLLA into a possible candidate for feedstock recycling plastics. However, the thermal degradation of PLLA is more complex than the simple reaction that gives L,L-lactide and involves the generation of significant amounts of other volatile decomposition products brought out during the pyrolysis [5,12,13]. The factors, which have been reported to influence PLLA thermal decomposition, include moisture, residual and hydrolyzed monomers, oligomers, molecular weight, and residual metals. In particular, the effect of the Sn atom is very important, because only Sn 2-ethylhexanoate {$Sn(Oct)_2$} has been approved by FDA as the catalyst [14].

Some reports about the effect of the Sn atom on the PLLA pyrolysis have been published. Jamshidi et al. reported the accelerating effect of $Sn(Oct)_2$ (5 wt%) on the PLLA pyrolysis with thermobalance (TG), in which the weight loss of PLLA was brought about even at temperature as low as 160^{O}C [15]. They showed in weight loss curves under isothermal conditions that the Sn-containing sample exhibited a linear weight loss curve with time, in contrast to the pure PLLA, which showed a sigmoid curve. One interpretation of

these results is that they suggest a change in the weight loss behavior from a random process to a zero-order reaction process by the addition of Sn atom. Södergård and Näsman also demonstrated that the addition (0.5 and 1.0 wt%) of $Sn(Oct)_2$ accelerated the melt degradation rate in an internal mixer, and suggested a mechanism that is a random main-chain scission, based on the parallel shift of the size exclusion chromatography profile [16]. Moreover, they also demonstrated the random scission of PLLA (Sn content: 690 ppm) based on a linear relationship between $1/\eta_{eff}^{0.3}$ and time, and derived the activation energy *Ea*=119.4 kJ mol^{-1} [17]. Kopinke et al. compared the weight loss behavior on pyrolysis of two types of PLLAs, in which the Sn contents were 15 and 250 ppm [18]. They reported the accelerating effect of the Sn atom and two dominating decomposition pathways, i.e., the first selective production of lactide at lower temperature and the second non-selective production of higher cyclic oligomers at higher temperature. They reported the same *Ea* value of 110 kJ mol^{-1} for both PLLA decomposition stages, this value having been tentatively calculated according to a 1^{st}-order kinetic treatment in the range of low conversion degree. Wachsen et al. also compared the thermal degradation behavior of the two types of PLLAs (Sn content: 15 and 145 ppm) in sealed ampoules, and the *Ea* values: 120 and 92 kJ mol^{-1} were calculated based on the random degradation and recombination equilibrium equations, respectively [19]. Noda et al. evaluated the activity of a series of Al, Ti, Zn, Zr, and Sn compounds as intramolecular transesterification catalysts, and reported that the activity of each metal was in the following order: Sn>Zn>Zr>Ti>Al [20]. Degée et al. also reported that PLLA prepared with $Sn(Oct)_2$ was less stable thermally than that prepared with Al alkoxides from TG data [21]. However, Cam and Marucci reported a contrary effect with the order: Fe>Al>Zn>Sn for

the PLLA thermal decomposition onset temperature on TG curve [22].

As mentioned in the previous reports, the accelerating effect of Sn atom on PLLA thermal degradation is clear, however it has not yet clearly been established whether the degradation mechanism is a 1st-order reaction or random reaction. The analysis is further complicated by changes in the mechanism in the course of the decomposition and many factors other than Sn content. Of course, it is well known that besides the Sn content there are many factors influencing the pyrolysis behavior as abovementioned. Therefore, to analyze the effect of the Sn atom accurately, all the experimental parameters other than the Sn content have to be kept as constant as possible. In this article, the molecular weight and the distribution of PLLA samples had a similar range, and the amount of Sn compound in the PLLA samples was controlled by an extraction manner from an original PLLA sample, which included plenty of the Sn atom as the catalyst residue. From dynamic pyrolysis of PLLA samples conducted on TG, the kinetics and changes in the course of its decomposition were discussed, based on the analyses with the integration, and random degradation analytical methods as compared with the simulation curves [23,24].

2. Experimental

2.1. Materials

Monomer, L-lactide, was obtained from Shimadzu Co. Ltd. It was composed of 99.4% L-lactide and 0.6% *meso*-lactide according to a gas chromatography (GC) measurement. This monomer was recrystallized three times from dry toluene, and then once from dry ethyl acetate. After the purification,

meso-lactide was not detectable by GC. The vacuum dried L-lactide was stored in an N_2 atmosphere. Catalyst, Sn 2-ethylhexanoate {$Sn(Oct)_2$}, obtained from Wako Pure Chemical Industries, Ltd. was distilled under reduced pressure before use. The ammonia solution (25%) and hydrochloric acid (1**M**) specifically produced for the atomic absorption spectrophotometry were purchased from Wako Pure Chemical Industries, Ltd. and used as received.

2.2. Preparation of poly (L-lactide) samples with different Sn contents

Poly(L-lactide) (PLLA) was synthesized by the ring-opening polymerization catalyzed by $Sn(Oct)_2$. A molar ratio, [catalyst]/[monomer]=1/2000, in feed and a multi-temperature process (150°C/0.5h + 130°C/5h + 110°C/13h + 90°C/12h) were employed in the polymerization. To prepare PLLA samples with different Sn contents, the Sn-catalyst residue was extracted from the as-polymerized PLLA/chloroform solution using a 1**M** HCl aqueous solution, then the polymer solution was washed with distilled water until the aqueous phase became totally neutral, and then finally the polymer was precipitated with methanol. The extraction/precipitation process was repeated a number of times to obtain the 7 PLLA samples with different Sn contents.

In the preparation of PLLA films, each chloroform solution of the PLLA sample was cast on the surface of a glass Petri dish. After the evaporation of the solvent, the formed film was washed by methanol and then vacuum dried.

2.3. Dynamic pyrolysis

Thermogravimetric analysis (TG/DTA) was conducted on a Seiko Instruments Inc. EXSTAR 6200 TG system in aluminium pans under a constant nitrogen flow (100 mL min^{-1}) using about 8 mg of the PLLA film sample. For each sample, prescribed heating rates of 1, 3, 5, 7, and 9 K min^{-1} were applied from room temperature to 400°C. The pyrolysis data were collected at regular intervals (about 20 times K^{-1}) by an EXSTAR 6000 data platform, and recorded into an analytical computer system.

2.4. Pyrolysis in glass tube oven

About 200 mg of the PLLA sample was put into a Shibata GTO-350D glass tube oven. After air was substituted for nitrogen in the chamber of the oven, the oven was heated gradually to 350°C and then kept at this temperature for 20min. The distilled components were collected and analyzed by gas chromatography (GC).

2.5. Measurements

The gas chromatography (GC) measurements were recorded on a Shimadzu GC-9A gas chromatograph with a Varian cyclodextrine-^{2} -236M-19 capillary column (0.25mm×50m) using helium as the carrier gas. The column and injector were set isothermally at 150 and 220ºC, respectively. The sample (3mg) was dissolved in acetone (1 mL) and a 1 μL aliquot of the solution was injected. The peaks for *meso*-, L,L-, and D,D-lactides were identified by comparison with pure substance peaks.

Gel permeation chromatography (GPC) was measured on a TOSOH HLC-8220 GPC system at 40ºC using TOSOH TSKgel Super HM-H column and chloroform eluent (0.6 mL min^{-1}). Low polydispersity polystyrene standards with *Mn* from 560 to 113,200 were used for calibration. The sample (12 mg) was dissolved in chloroform (2 mL) and the solution was filtered through a membrane filter having a 0.5 μm pore size.

The Sn content in the PLLA samples was measured with a Shimadzu AA-6500F atomic absorption flame emission spectrophotometer (AA). The sample was degraded by a 25% ammonia solution, dissolved in 1**M**-hydrochloric acid, and then measured by AA.

Pyrolysis-gas chromatograph/mass spectra (Py-GC/MS) were recorded on a Frontier Lab double-shot pyrolyzer PY-2020D with a Frontier Lab SS-1010E selective sampler and a Shimadzu GCMS-QP5050 chromatograph/mass spectrometer. High purity helium was used as carrier gas at 50mL min^{-1}. The volatile products were analyzed with an Ultra $Alloy^{+}$-5 capillary column (30m x 0.25mm i.d.; film thickness, 0.25μm). A PLLA sample was put in the pyrolyzer and heated from 40 to 400ºC at a heating rate of 9ºC min^{-1}. The volatile pyrolysis products were conducted into the GC through the selective sampler. The temperature of column oven was first set at 40°C. After the pyrolysis process had finished, the column was heated according to the following program: 40ºC for 5 min; 40-320ºC at 20ºC min^{-1}; 320°C for 30 min. Mass spectrum measurements were recorded 2 times s^{-1} during this period.

3. Results and Discussion

3.1. Preparation of PLLA samples with different Sn contents (PLLA-Sn)

PLLA was synthesized through the ring-opening polymerization catalyzed by Sn 2-ethylhexanoate {$Sn(Oct)_2$}. After the polymerization, Sn content in the PLLA was controlled by repeating the liquid-liquid extraction process using a 1**M** HCl aqueous solution. Number and weight average molecular weights (*Mn* and *Mw*) and Sn content of the obtained PLLA samples (PLLA-Sn) were listed in Table 1. The *Mn*, *Mw*, and Sn content of the original as-polymerized PLLA (Sn-607) were 99,800, 158,000, and 607 ppm, respectively. Considering the Mark-Houwink-Sakurada constants for PLLA [25], the Sn content corresponds to 49.5% of the number of chain ends. As a function of the number of times of extraction, the Sn content was found to decrease stepwise to 20 ppm, whereas the *Mn* and *Mw* were maintained in the ranges of 76,000-104,500 and 121,300-158,000, respectively.

Thus, though the chemical structures of residual Sn compounds are not yet clear [9], the PLLA-Sn samples should include similar residual Sn species.

Table 1 goes here

3.2. Pyrolysis products from PLLA-Sn

Pyrolysis products were determined by the pyrolysis-gas chromatography/mass spectrometry (Py-GC/MS). In Figure 1, the total ion chromatograms (TIC) of the evolved gas from PLLA samples, Sn-20 and Sn-607, in the temperature range 40-400°C are illustrated. The Py-GC/MS (TIC) spectrum of Sn-20 showed main peaks for lactides in the range of 8-10 min of the retention time and minor peaks for

higher cyclic oligomers in the range of 15-22 min (Figure 1a). The spectrum was nearly the same as that of the purified PLLA (Sn content: 9 ppm) reported previously [26]. As discussed in previous reports, the main peaks at 9.25 and 9.73 min represented *meso*-lactide and D,D-/L,L-lactides, respectively, and the intensity ratio of *meso*-form to total lactides was 36.8%. Each group of peaks appearing periodically after 15 min was assigned to a group of diastereoisomers of one kind of higher cyclic oligomer, which was in the range from trimer to heptamer [5,18,26]. Summation of the integrated intensity of these oligomer peaks was 20.5 % of the total intensity. In contrast to the spectrum of Sn-20, the Py-GC/MS (TIC) spectrum of Sn-607 (Figure 1b) indicated a dominant peak for the D,D-/L,L-lactides (meso: D,D/L,L = 11.4:88.6 in intensity ratio). The production of oligomers higher than lactide was obviously decreased to 0.9 % of the total intensity. The high L,L-lactide selectivity on Sn-catalyzed oligo(L,L-lactide) pyrolysis has already been reported by Noda et al. [20].

Volatile degradation products were also collected from the isothermal pyrolysis at 350ºC in a glass tube oven and analyzed by gas chromatography (GC) with a capillary column, cyclodextrin-β-236M-19. As a result, the volatile products from Sn-607 were dominated by lactides (*meso*:D,D:L,L = 5.90:1.23:92.87) with only 0.2% of lower boiling point products in the retention time range of 5-12 min. In contrast the volatile products from the purified PLLA included 14.5% of lower boiling point products.

These results indicate that residual Sn compounds effect the pyrolysis by causing the selective elimination of lactide, which means that the pyrolysis pathway of Sn-rich PLLA may be relatively simple.

Figure 1 goes here

3.3. Dynamic pyrolysis of PLLA-Sn and kinetics

To analyze the thermal degradation behavior of PLLA-Sn, the dynamic thermal degradation was examined by measuring the weight loss of the film samples as a function of linear increase in temperature in a nitrogen atmosphere using TG. The TG curves of the PLLA-Sn samples at a heating rate of ϕ = 5K min^{-1} are shown in Figure 2. All the curves show nearly complete degradation and with increase in Sn content the curve shifted toward a lower temperature range. The residual Sn compounds clearly enhanced the thermal degradation of PLLA similarly to previous reports [15-22].

Figure 2 goes here

The kinetic parameters of PLLA-Sn pyrolysis were evaluated from the thermogravimetric data. In this study the well-known integral method and an improved random degradation analytical method [23,24,27-33] were employed to analyze the pyrolysis data of PLLA-Sn. The dynamic decomposition of PLLA-Sn samples was carried out at different heating rates ϕ ranging from 1-9 K min^{-1}, and the kinetic parameters were estimated according to the same procedure as mentioned in a previous report [24]. At a certain fractional weight ratio *w*, the apparent activation energy *Ea* was calculated from the slope of a $\log(\phi)$ vs. $1/T$ plot. The apparent *Ea* values were re-calculated using the corrected *a* and *b* values, in which *a* and *b* are constant values in Doyle's approximation equation [27,28].

Figure 3 shows changes in the apparent *Ea* value with *w*. Each sample exhibited a characteristic curve. The curves of Sn-20 and Sn-34 started from *Ea* = 135 kJ mol^{-1} and gradually increased to converge

at 180-190 kJ mol^{-1}. This change in the *Ea* value is almost the same as that of the purified PLLA reported previously [26]. In the case of Sn-60, the *Ea* value increased gradually from 125 to 165 kJ mol^{-1}. The *Ea* values of Sn-168 and Sn-396 pyrolysis were kept constant at 120-125 kJ mol^{-1}, but increased a little in the last period. The pyrolysis of Sn-485 and Sn-607 also kept the *Ea* value at about 115-125 kJ mol^{-1}, decreasing finally to 105-110 kJ mol^{-1}. These different *Ea* curves indicate that the degradation process gradually changes according to the Sn content and weight loss in each sample. This frequently observed *Ea* value of around 120 kJ mol^{-1} is close to the 119.4 kJ mol^{-1} reported by Södergård and Näsman [17], but at odds with the 92 kJ mol^{-1} reported by Wachsen et al. [19].

Figure 3 goes here

In Figure 4, the random degradation analysis plots of $\log[-\log\{1-(1-w)^{1/2}\}]$ vs. $1/T$ for PLLA Sn-20 (1 K min^{-1}) and model reactions are illustrated. The model reaction simulations for the random degradations exhibit nearly linear relationships [24]. On the other hand, each n^{th}-order model reaction simulation is represented by a characteristic curve. The experimental data plot obviously conformed to the n^{th}-order reaction simulations with parameter values: activation energy *Ea*=135 kJ mol^{-1} and pre-exponential value $A=3.4\times10^{8}$ s^{-1} at the initial stage, and then shifted to the random reaction simulations with *L*=3~5, where *L* means the least number of repeating units of oligomer not volatilized [31]. The integral analysis plots for PLLA Sn-20 (9 K min^{-1}) and model reactions are illustrated in Figure 5. In this Figure, $\theta=(AEa/\phi R)p(y)$ is defined as the reduced time [23]. The main reaction of Sn-20 (9 K min^{-1}) was approximated by a random degradation *L*=4 with parameter values: *Ea*=185 kJ mol^{-1} and $A=7.5\times10^{12}$ s^{-1}, which is similar to the

degradation of the purified PLLA [26]. This increase in the *L* value agrees with the higher oligomer production detected in the Py-GC/MS spectrum (Figure 1a).

At least two speculative explanations should be considered for the overlap on the n^{th}-order reaction simulation in the initial period. One is an n^{th}-order reaction caused by Sn atoms at a lower temperature. Kopinke et al. suggested that the initial degradation process in a lower temperature range of a Sn-rich PLLA (Sn content: 250ppm) would be a Sn-catalyzed depolymerization starting from free hydroxyl groups at chain ends. This explanation, however, did not deal with Sn-poor PLLA (Sn content: 15 ppm) [18]. The other explanation refers to an evaporation process of cumulated volatile products by pre-decomposition reactions taking place before detection of the weight loss. Random chain scission of PLLA at low temperature also has been reported in some literature [17,19]. In fact, it was confirmed that the evaporation of L,L-lactide represented a zero-order weight loss behavior in the same thermal process with TG (data not shown).

Figure 4 goes here

Figure 5 goes here

In the case of PLLA Sn-60 (1 K min^{-1}), the n^{th}-order weight loss behavior in the initial period was reduced and shifted closer to the simulation plots for random degradations. This shift may quash the speculation of the Sn-catalyzed depolymerization occurring at lower temperatures, whilst supporting the other speculation, regarding the evaporation process of cumulated products, because it is reasonable to suppose that the shift to a lower temperature range depresses the production, accumulation, and evaporation

of pyrolyzates, resulting in the divergence from the n^{th}-order reaction simulation curves. In later stages of the degradation, a shift of the plot to other random degradation simulations with higher *L* values was found to be similar to the manner of the Sn-20 pyrolysis process.

The result of the random degradation analysis of Sn-169 pyrolysis data (1 K min^{-1}) showed a typical initiation process through a random degradation (*L*=3) manner with parameter values: *Ea*=122 kJ mol^{-1} and *A*=0.9x10^{8} s^{-1}, without any initial n^{th}-order reaction behavior. In Figure 6, the main degradation process of Sn-169 (9 K min^{-1}) was plotted tentatively with parameter values: *Ea*=123 kJ mol^{-1} and *A*=1.0x10^{8} s^{-1}, and compared to the model reactions. These model simulations did not approximate to the main period of the experimental data plot. However, a rapid weight loss curve after the initial random degradation could be regarded as being in parallel to a zero-order model simulation. This suggests a mechanistic change into a zero-order weight loss process.

Figure 6 goes here

When the Sn content increased up to 607 ppm, the initial degradation of Sn-607 (1 K min^{-1}) proceeded on a simulation plot of random degradation (*L*=3) with parameter values: *Ea*=119 kJ mol^{-1} and *A*=2.0x10^{8} s^{-1} and thereafter rapidly shifted away from the random (*L*=3) simulation with an associated rise in *L* value (*L*~9) (Figure 7). The illustrated plot in Figure 8 is the data plot of Sn-607 (1 K min^{-1}) by the integral method with parameter values: *Ea*=119 kJ mol^{-1} and *A*=4.0x10^{8} s^{-1}. Interestingly, after the random process in the initial period, the weight loss curve showed a linear relationship between *w* and $A\theta$ in parallel to the zero-order simulation plot. The Py-GC/MS spectrum in Figure 1b supports the zero-order

reaction, but not the random degradation (L>3). The same degradation behavior was also determined from the simulation analysis of Sn-607 (9 K min^{-1}) and PLLA Sn-485 pyrolysis data.

According to Flynn and Wall [32], if the total material may be volatilized by two alternative paths, for which the respective Arrhenius parameters are Ea_1 and A_1 and Ea_2 and A_2, and if the two paths are expressible by a combined function $f(w)$, then the integration will be given by

$$-\int \frac{dw}{f(w)} = \frac{A_1}{\phi}\int \exp(-Ea_1/RT) + \frac{A_2}{\phi}\int \exp(-Ea_2/RT)$$

$$= \frac{A_1 Ea_1}{\phi R}\,p(x_1) + \frac{A_2 Ea_2}{\phi R}\,p(x_2) = A_1\theta_1 + A_2\theta_2$$

where x_1, x_2, θ_1, and θ_2 are Ea_1/RT, Ea_2/RT, $(Ea_1/\phi R)p(x_1)$, and $(Ea_2/\phi R)p(x_2)$. If the two paths occur at different temperature ranges, the paths may appear as consecutive reactions. This equation supports the linear relation parallel to the zero-order simulation plot being regarded as a zero-order reaction. Thus, the time lag, $A_1\theta_1$, between the linear part of the experimental plot and the zero-order simulation plot in Figure 8 is regarded as a retardation time or induction period to shift into the zero-order reaction from the initial random degradation process shown in Figure 7.

The obtained kinetic parameters on the pyrolysis of PLLA-Sn samples are listed in Table 2. Obviously, the Sn-catalyzed pyrolysis of PLLA starts through the random degradation (L=3) behavior, and then shifts to the zero-order weight loss process. The details of the mechanistic change are discussed in the next section.

Figure 7 goes here

Figure 8 goes here

Table 2 goes here

3.4. Mechanism of PLLA-Sn pyrolysis

In this Sn-catalyzed PLLA pyrolysis, the initial random degradation behavior and the change in the process with the weight loss were clearly shown. The initial degradation behavior must be due to the Sn-catalyzed random transesterification. The estimated changes in degradation process are represented as a result of the shift to zero-order weight loss process from the random degradation process. The observed linear relationship between w and $A\theta$ and the selective production of lactides for Sn-rich PLLA samples are successfully explainable by the zero-order weight loss process. The zero-order weight loss process via initial random degradation process can be achieved by two possible degradation routes, namely the cooperation of an unzipping depolymerization into a random transesterification reaction continuing from the initial stage, or alternatively a shift to a pseudo-selective lactide elimination depending on Sn atom-content from an initial random transesterification reaction (Scheme 1a and 1b). Kopinke et al. suggested the Sn-catalyzed selective depolymerization from free hydroxyl end groups [18]. However, it should be noted that the unzipping depolymerization of polymer with polydispersity index ~2 results in 1^{st}-order weight loss behavior. To show the zero-order weight loss behavior under the unzipping depolymerization process, a cooperative random transesterification is indispensable (Scheme 1a). In this process, the PLLA can be regarded as a monodispersive polymer apparently, mirroring the pyrolysis behavior of poly(*p*-dioxanone) [34]. In this case, the chain end structure is likely to be a Sn-alkoxide during

the unzipping depolymerization process. On the other hand, the Sn-catalyzed pseudo-selective lactide elimination may occur in cumulated flexible oligomers, in which an effective Sn-catalyzed transesterification reaction between neighboring units may result in pseudo-selective lactide elimination (Scheme 1b). The fact that the *Ea* value remains constant despite the change in the manner of degradation may support this view.

Another possible view proposes a simple reaction (Scheme 1c). In this process, the Sn-catalyzed selective lactide elimination by Sn atom combined at the polymer chain-end is assumed to be a fundamental reaction. The reaction may be controlled by the mobility of Sn salt moiety, thus the reaction may be delayed depending on the molecular weight of the polymer chain, exhibiting an apparent weight loss behavior in the same way as a random reaction in the initial period.

The value of the contributions of each of the abovementioned speculations on the PLLA-Sn pyrolysis is not yet clear, but recent examinations to clarify the subject are in progress.

Scheme 1 goes here

4. Conclusions

To clarify the effect of residual Sn atom on the PLLA pyrolysis, PLLA samples with different Sn contents from 20-607 ppm were prepared maintaining a similar level in both molecular weight and distribution. The PLLA Sn-607 was subjected to pyrolysis in the temperature range of 40-400°C to produce lactides selectively. This is in contrast to that of PLLA Sn-20, which was accompanied by the production of

cyclic oligomers. The dynamic pyrolysis of PLLA-Sn samples was conducted in TG cells. The increase in Sn content moved the degradation temperature to a lower range, and caused the activation energy *Ea* to decrease and converge at about 120 kJ mol^{-1}. From the kinetic analysis of the dynamic pyrolysis data, it was determined that the Sn-catalyzed pyrolysis of PLLA starts through a random degradation (L=3) behavior and then shifts to a zero-order weight loss process. Three possible zero-order reactions were postulated, one being the cooperation of an unzipping reaction with a random transesterification reaction, and the other two being Sn-catalyzed pseudo-selective and selective lactide eliminations from a random site on a polymer chain with dependence on the Sn atom-content.

References

[1] Ikada Y, Tsuji H. Biodegradable polyesters for medical and ecological applications. Macromol Rapid Commun 2000; 21(3): 117-32.

[2] Amass W, Amass A, Tighe B. A review of biodegradable polymers: Uses, current developments in the synthesis and characterization of biodegradable polyesters, blends of biodegradable polymers and recent advances in biodegradation studies. Polym Int 1998; 47(2): 89-144.

[3] Anderson JM, Shive MS. Biodegradation and biocompatibility of PLA and PLGA microspheres. Advan Drug Delivery Rev. 1997; 28 (1): 5-24.

[4] Ajioka M, Enomoto K, Suzuki K, Yamaguchi A. The basic properties of poly (lactic acid) produced by the direct condensation polymerization of lactic acid. J Environm Polym Degrad 1995; 3(4): 225-34.

[5] Khabbaz F, Karlsson S, Albertsson AC. Py-GC/MS an effective technique to characterizing of degradation mechanism of poly (L-lactide) in the different environment. J Appl Polym Sci 2000; 78: 2369-78.

[6] Pranamuda H, Tokiwa Y, Tanaka H. Polylactide Degradation by an *Amycolatopsis* sp. Appl Environ Microbiol 1997; 63: 1637-40.

[7] Lunt J. Large-scale production, properties and commercial applications of polylactic acid polymers. Polym Degrad Stab 1998; 59: 145-52.

[8] Leenslag JW, Pennings AJ. Synthesis of high-molecular-weight poly(L-lactide) initiated with tin 2-ethylhexanoate. Makromol Chem 1987; 188: 1809-14.

[9] Kricheldorf HR, Kreiser-Saunders I, Stricker A. Polylactones 48. $SnOct_2$-initiated polymerization of lactide: a mechanistic study. Macromolecules 2000; 33: 702-9.

[10] Duda A, Penczek S. Thermodynamics of L-lactide polymerization. Equilibrium monomer concentration. Macromolecules 1991; 23: 1636-9.

[11] Witzke DR, Narayan R. Reversible kinetics and thermodynamics of the homopolymerization of L-lactide with 2-ethylhexanoic acid tin(II) salt. Macromolecules 1997; 30: 7075-85.

[12] Leiper HA, McNeill IC. Degradation studies of some polyeaters and polycarbonates-2. Polylactide: Degradation under isothermal conditions, thermal degradation mechanism and photolysis of the polymer. Polym Degrad Stab 1985; 11: 309-26.

[13] Kopinke, FD, Mackenzie K. Mechanism aspects of the thermal degradation of poly(lactic acid) and poly (² -hydroxybutyric acid). J Anal Appl Pyrol 1997; 40-41: 43-53.

[14] Food Drug Adm. Food additives. Resinous and polymeric coatings. Fed Regist 1975; 40(121) C (23. Jun 1975) (CA 83: 112493h).

[15] Jamshidi K, Hyon SH, Ikada Y. Thermal characterization of polylactides. Polymer 1988; 29: 2229-34.

[16] Södergård A, Näsman JH. Stabilization of poly(L-lactide) in the melt. Polym Degrad Stab 1994; 46: 25-30.

[17] Södergård A, Näsman JH. Melt stability study of various types of poly(L-lactide). Ind Eng Chem Res 1996; 35: 732-5.

[18] Kopinke FD, Remmler M, Mackenzie K, Moder M, Wachsen O. Thermal decomposition of biodegradable polyesters-II. Poly (lactic acid). Polym Degrad Stab 1996; 53: 329-42.

[19] Wachsen O, Platkowski K, Reichert KH. Thermal degradation of poly-L-lactide – studies on kinetics, modeling and melt stabilization. Polym Degrad Stab 1997; 57: 87-94.

[20] Noda M, Okuyama H. Thermal catalytic depolymerization of poly(L-lactic acid) oligomer into L,L-lactide: Effects of Al, Ti, Zn, and Zr compounds as catalysts. Chem Pharm Bull 1999; 47: 467-71.

[21] Degée P, Dubois P, Jérôme R. Bulk polymerization of lactides initiated by aluminium isopropoxide, 3

Thermal stability and viscoelastic properties. Macromol Chem Phys 1997; 198: 1985-95.

[22] Cam D, Marucci M. Influence of residual monomers and metals on poly(L-lactide) thermal stability. Polymer 1997; 38: 1879-84.

[23] Ozawa T. A new method of analyzing thermogravimetric data. Bull Chem Soc Japan 1965; 38:1881-6.

[24] Nishida H, Yamashita M, Endo T. Analysis of initial process in pyrolysis of poly (*p*-dioxanone). Polym Degrad Stab 2002; 78: 129-135.

[25] Witzke DR, Narayan R, Kolstad JJ. Reversible kinetics and thermodynamics of the homopolymerization of L-lactide with 2-ethylhexanoic acid Tin(II) salt. Macromolecules 1997; 30: 7075-85.

[26] Fan Y, Nishida H, Hoshihara S, Shirai Y, Tokiwa Y, Endo T. Pyrolysis kinetics of poly(L-lactide) with carboxyl and calcium salt end structures. Polym Degrad Stab. in press.

[27] Doyle CD. Kinetics analysis of thermogravimetric data. J Appl Polym Sci 1961; 5: 285-92.

[28] Doyle CD. Estimating isothermal life from thermogravimetric data. J Appl Polym Sci 1962; 6: 639-42.

[29] Flynn JH, Wall LA. A quick, direct method for the determination of activation energy from thermogravimetric data. Polym Lett 1966; 4: 323-8.

[30] Reich L. A rapid estimation of activation energy from thermogravimetric traces. Polym Lett 1964; 2: 621-3.

[31] Simha R, Wall LA. Kinetics of chain depolymerization. J Phys Chem 1952; 56: 707-15.

[32] Flynn JH, Wall LA. General treatment of the thermogravimetry of polymers. J Res Nat Bur Stand 1966; 70A: 487-523.

[33] Ichihara S, Nakagawa H, Tsukazawa Y. Thermal decomposition behaviors of polymers analyzed with thermogravimetry. Kobunshi Ronbunshu 1994; 51(7): 459-65.

[34] Nishida H, Yamashita M, Hattori N, Endo T, Tokiwa Y. Thermal decomposition of poly(1,4-dioxan-2-one). Polym Degrad Stab 2000; 78: 485-96.

Table 1. PLLA samples with different Sn content (PLLA-Sn)

Sample	Sn content ppm	*Mn*	*Mw*
Sn-607	607	99,800	158,000
Sn-485	485	96,300	151,500
Sn-396	396	104,500	153,700
Sn-169	169	100,600	155,700
Sn-60	60	87,700	138,000
Sn-34	34	76,000	121,300
Sn-20	20	76,300	126,000

Table 2. Kinetic parameters for PLLA-Sn pyrolysis

Sample	Initial stage (w~0.9)			Main stage		
	Ea kJ mol^{-1}	*A* s^{-1}	*n / random*	*Ea* kJ mol^{-1}	*A* s^{-1}	*n / random*
Sn-607	119	2.0×10^8	random (L =3)	119	4.0×10^8	n = 0
Sn-485	121	2.2×10^8	random (L =3)	122	8.0×10^8	n = 0
Sn-396	123	1.3×10^8	random (L =3)	124	2.2×10^8	n^{th} + random
Sn-169	122	0.9×10^8	random (L =3)	123	1.2×10^8	random + n^{th}
Sn-60	130	2.0×10^8	random + n^{th}	(150)[a]	1.45×10^{10}	random + n^{th}
Sn-34	135	3.8×10^8	n^{th} + random	182	4.3×10^{12}	random (L =4)
Sn-20	135	3.4×10^8	n^{th}	185	7.5×10^{12}	random (L =4)

[a] Teatative value at w = 0.5.

Figure and Scheme Captions

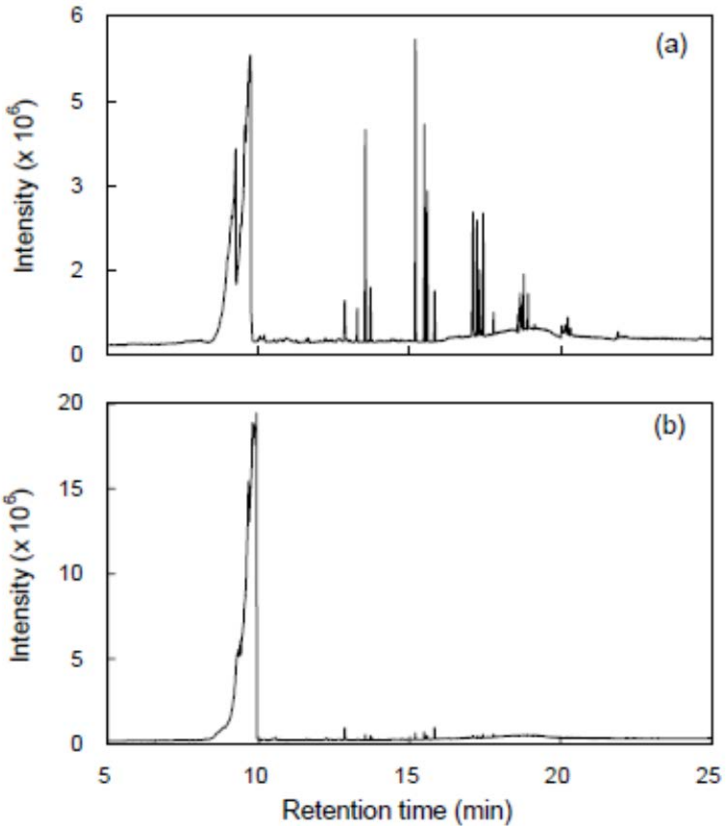

Figure 1. Py-GC/MS total ion current spectra of PLLA Sn-20 (a) and Sn-607 (b) pyrolysis products from 40 to 400˚C.

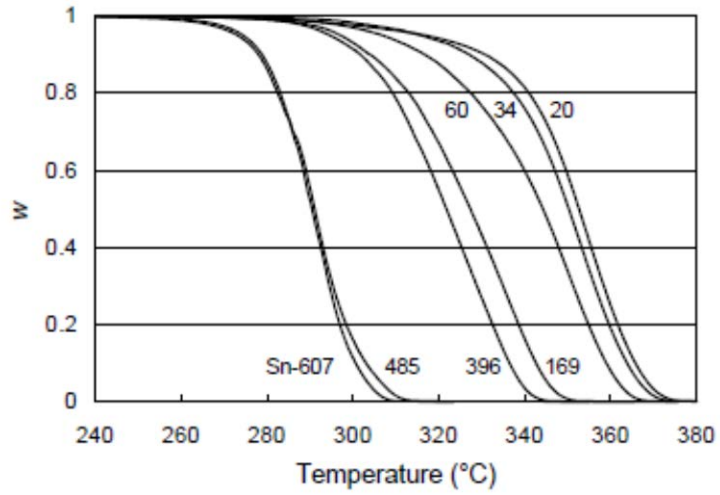

Figure 2. Thermogravimetric pyrolysis curves of PLLA-Sn samples at a heating rate of 5 K min^{-1} under N_2 flow of 100 mL min^{-1}.

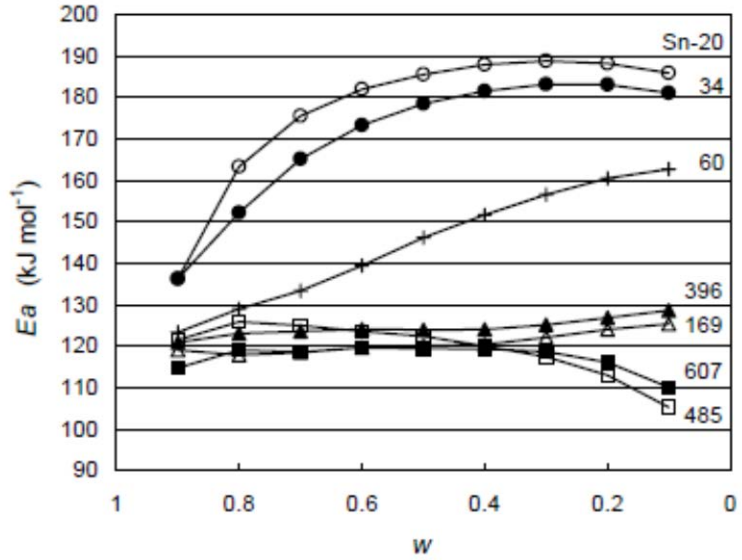

Figure 3. Apparent activation energies (*Ea*) at various residual weight fractions evaluated for PLLA Sn samples.

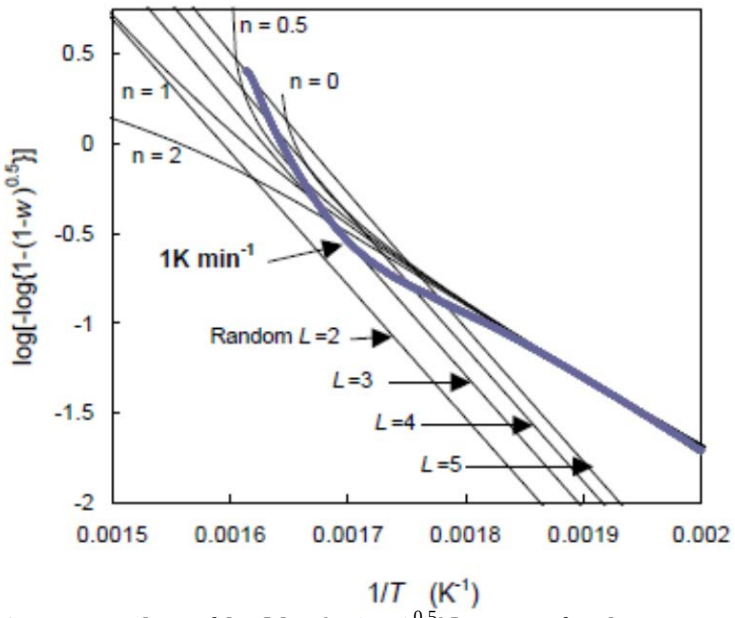

Figure 4. Plots of log[-log{1-(1-*w*)$^{0.5}$}] vs. 1/*T* for thermogravimetric data of PLLA Sn-20 at a heating rate of 1 K min^{-1} (*Ea*=135 kJ mol^{-1}, *A*=3.4×10^{8} s^{-1}), and for model reactions. Model reactions: zero (n=0), half (n=0.5), 1st (n=1), and 2nd-order (n=2), and random degradations (Random *L*=2-5).

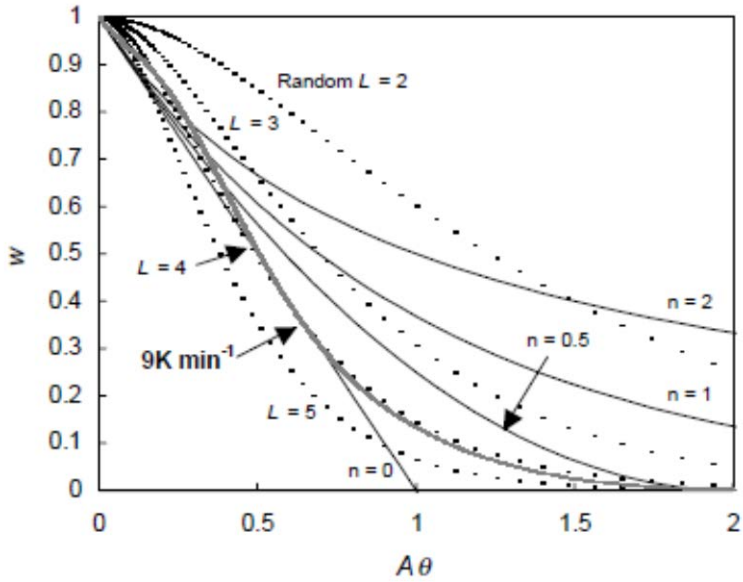

Figure 5. Plots of experimental $(AEa/\phi R)p(y)$ $(=A\theta)$ vs. w of PLLA Sn-20 at a heating rate 9 K min^{-1} (Ea=185 kJ mol^{-1}, A=7.5×10^{12} s^{-1}), and $-\int dw/g(w)$ vs. w for model reactions. Model reactions: zero (n=0), half (n=0.5), 1st (n=1), and 2nd-order (n=2), and random degradations (Random L=2-5).

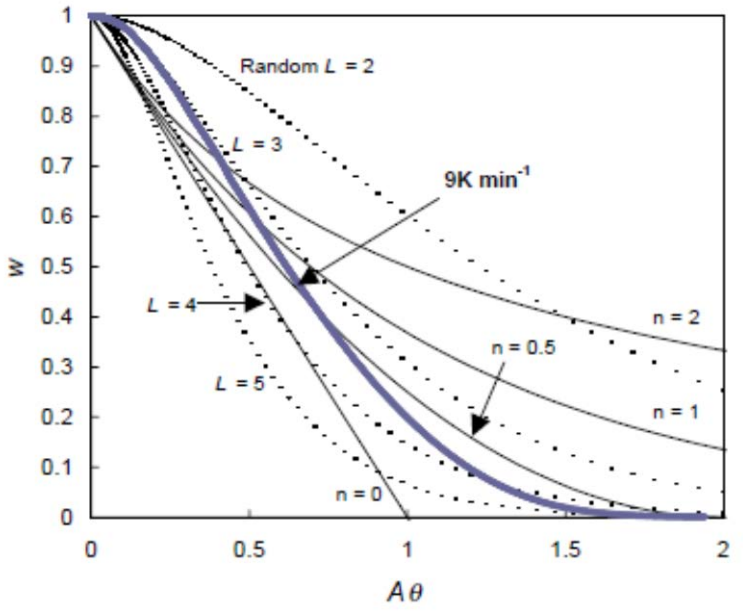

Figure 6. Plots of experimental $(AEa/\phi R)p(y)$ $(=A\theta)$ vs. w of PLLA Sn-169 at a heating rate 9 K min^{-1} (Ea=123 kJ mol^{-1}, A=1.2×10^{8} s^{-1}), and $-\int dw/g(w)$ vs. w for model reactions. Model reactions: zero (n=0), half (n=0.5), 1st (n=1), and 2nd-order (n=2), and random degradations (Random L=2-5).

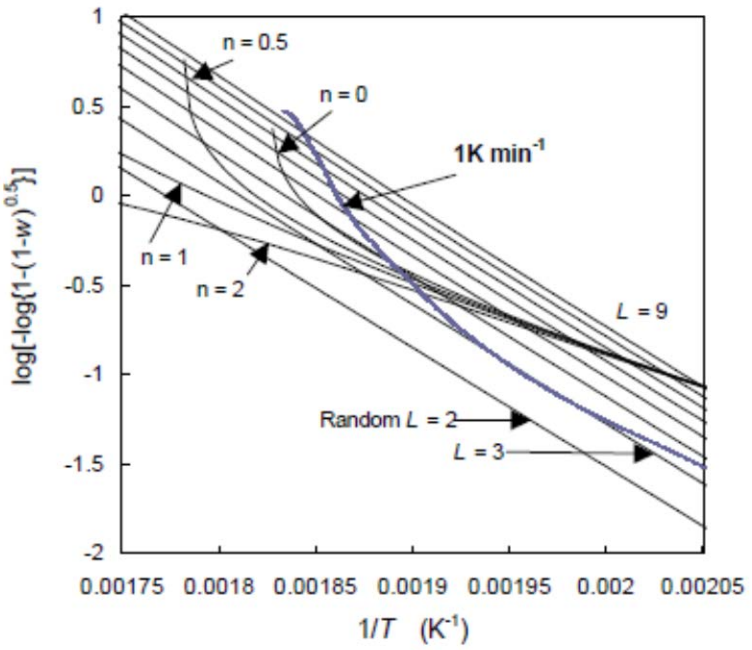

Figure 7. Plots of log[-log{1-(1-w)$^{0.5}$}] vs. 1/T for thermogravimetric data of PLLA Sn-607 at a heating rate of 1 K min^{-1} (Ea=119 kJ mol^{-1}, A=2.0×10^{8} s^{-1}), and for model reactions. Model reactions: zero (n=0), half (n=0.5), 1st (n=1), and 2nd-order (n=2), and random degradations (Random L=2-9).

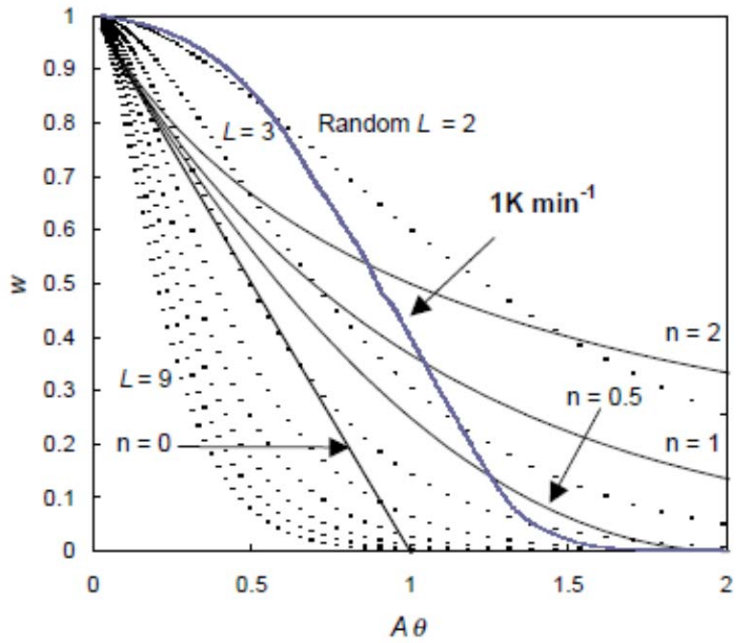

Figure 8. Plots of experimental ($AEa/\phi R$)p(y) (=$A\theta$) vs. w of PLLA Sn-607 at a heating rate 1 K min^{-1} (Ea=119 kJ mol^{-1}, A=4.0×10^{8} s^{-1}), and $-\int dw/g(w)$ vs. w for model reactions. Model reactions: zero (n=0), half (n=0.5), 1st (n=1), and 2nd-order (n=2), and random degradations (Random L=2-9).

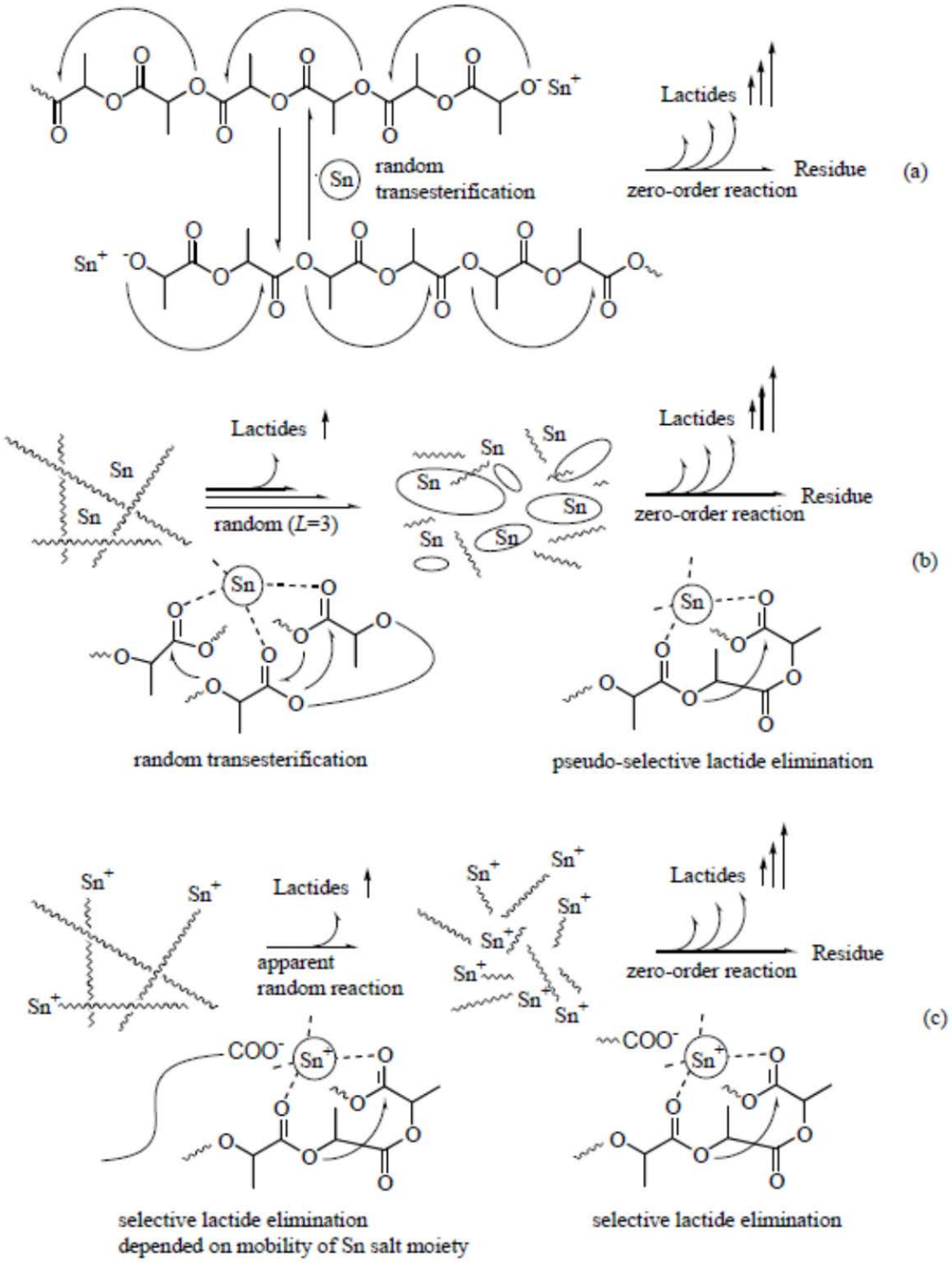

Scheme 1. Possible mechanisms of Sn-catalyzed PLLA thermal decomposition.